ISSN 1070-4272, Russian Journal of Applied Chemistry, 2021, Vol. 94, No. 8, pp. 1153–1162. © Pleiades Publishing, Ltd., 2021.

MACROMOLECULAR COMPOUNDS AND POLYMERIC MATERIALS

Aqueous Reversible Addition-Fragmentation Chain Transfer (RAFT) Polymerization: Synthesis, Properties, and Application of an Amphoteric Superplasticizer

Haiyue Wang[a],*, Zezhong Jiang[a], Liying Guo[a],, Rongrong Zheng[a], Jixin Li[a], Zhiguo Yao[a], and Lining Shan[a]**

[a]*School of Petrochemical Engineering, Shenyang University of Technology, Liaoyang, 111003 China*
**e-mail: albert_why@163.com*
***e-mail: lyguo1981@163.com*

Received May 25, 2021; revised October 8, 2021; accepted October 11, 2021

Abstract—In this paper, we report a more simple and efficient way to a maleimide-structural copolymer superplasticizer(SP) that was synthesized by aqueous reversible addition-fragmentation chain transfer(RAFT) polymerization of methylallyl sulfonate (SMAS), *N*-carbamoyl maleimide (NCM), and *N*-methoxy polyethylene glycols-*N*'-carbamoyl maleimide (MPNCM) . The structure was manifested by FTIR, ^{1}H NMR, TGA and GPC. The comonomers content of the SP were changed by the proportion of SMAS, NCM, and MPNCM in the synthesis recipes. The effects on fluidity, adsorption, zeta potential, compressive strength, scanning electron microscopy (SEM), and Isothermal calorimetry in cement mortars were investigated. The experimental result showed that the SP2 with the certain monomer ratio of SMAS, NCM, and MPNCM had excellent workability of concrete, dispersion, and retention capability. The positive and negative charges of the SP2 interacted with the charges of the surface of cement pastes were largely responsible for enhancing the flocculation of cement particles with the effects of repulsion of stereo hindrance forming. The saturated adsorption amount changes with the various proportions of SMAS, NCM, and MPNCM on account of the different ratios of the negative and positive charges on the cement particles. The proper ratio of comonomers of SP2 was benefiting the adsorption.

Keywords: adsorption; RAFT; plasticizer; grafting; dispersion

DOI: 10.1134/S1070427221080176

INTRODUCTION

The superplasticizers could improve the performance of concrete significantly, and also lead to an increase in concrete construction [1, 2]. Nowadays, superplasticizers were defined as the third generation high-performance superplasticizer, which have been broadly utilized in concrete construction and assumed a noteworthy part of cement building [3–5]. The researchers design the molecular structure according to the mechanism of action in two areas. On the one hand, the superplasticizers are synthesized with polar groups, such as carboxyl groups, hydroxyl and sulfonic acid groups, and so on. Those groups can increase the dispersibility of the cement particles forming interaction between Ca^{2+} cations and other anions [6]. On the other hand, the superplasticizers are synthesized with active long chains, such as polyoxyethylene ether and so on. Those hydrophilic chains could increase dispersing performance and slump retention ability of superplasticizers by changing the space steric [7]. Lingfei Jiang et al. prepared a series of amphoteric superplasticizers by radical copolymerization of vinyl monomers and two cationic monomers [2, 3, 8]. The result shows that the superplasticizers could effectively adsorb on the surface of cement pastes. Ahmad Habbaba et al. reported the performance of polycarboxylate synthesis by allyl maleate, maleic anhydride, and allyl ether macromonomer. The result shows that the new intermolecular interaction generates a higher affinity

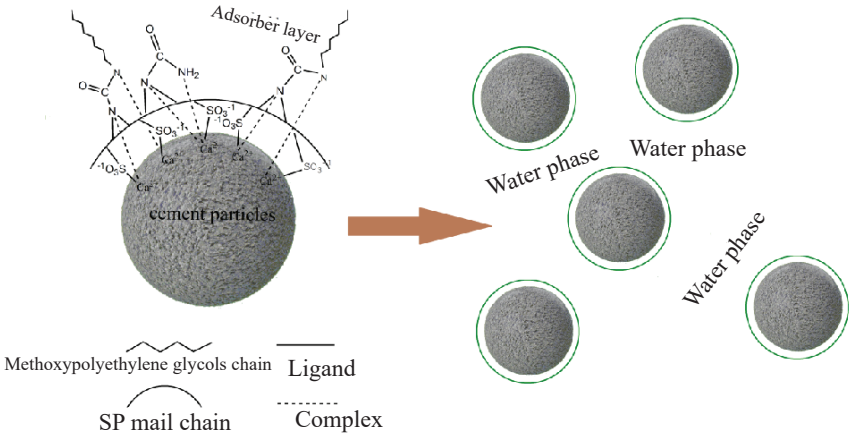

Fig. 1. The mechanism of action.

of the superplasticizers to the surface of cement and can form a denser adsorption layer [9]. To date, most chemical admixtures were called anionic admixture. Something else, such as amphoteric or cationic compounds, has been little available. Many amphoteric polymers (PACs) have a better effect on dispersing compound powder in water. Besides, the performance of such polymers would be changed, such as the fluidity.

Nonetheless, the factor of influence of the molecular structure on the mechanism of action of PAC is still indefinable. The cause is possible that it is the obstacles for the researchers to prepare the suitably molecule-design PAC [10, 11]. Consequently, one of the fundamental assumptions in the study of the PAC molecular structure has been only altered one component successfully, while the rest of the structure remains stationary according to main adsorption mechanisms:electrostatic adsorption and interlayer adsorption [12]. In these cases, theoretical scarcities hinder the development of further research on the PACs. He etal find comparing with traditional, introducing the ILs to superplasticizers can be preferentially absorbed by the surface electrostatic between cationic ILs and cements [13]. Qian report that the superplastics bring about great adsorption by electrostatic repulsion between hydrophobic groups into chains and cements [14]. The mechanism of action is probable shown in Fig. 1.

The reversible addition-fragmentation chain-transfer (RAFT) polymerization offers a feasibility route to solve the aforementioned problems thoroughly [15, 16]. The RAFT polymerization could acquire functional PACs with the designed molecular weight and well molecular weight distribution. This synthetic method has been widely employed by the extensive range of applications for styrene, acrylate and vinyl monomers, etc. [17–22]. superplasitizer monomer synthesized by aqueous RAFT is less common [23, 24].

To provide accurate insights, we have evaluated the maleimide-structural copolymer superplasticizer(SP) by RAFT polymerization in this work. This is the first study that reports SP is synthesized by aqueous RAFT of methylallyl sulfonate (SMAS), *N*-carbamoylmaleimide (NCM), and *N*-methoxy polyethylene glycols-*N*'-carbamoyl maleimide (MPNCM). In this study, 4-cyanopentanoic acid dithiobenzoate (CTA) was synthesized as RAFT agent. The structure of the SP was manifested by FT-IR, ^{1}H NMR, TGA and GPC. The fluidity, adsorption, compressive strength, Zeta potential of SP electron microscopy (SEM), and Isothermal calorimetry in cement mortars were studied.

EXPERIMENTAL

Materials

Maleic anhydride (MAH), methoxy polyethylene glycol (MPEG, Mn: 500), ammonium persulfate (APS), carbamide (UREA), methylallyl sulfonate (SMAS), methylbenzene (MB), ethanol (ET), triarylphosphines (PPh_3), ethylene diamine tetraacetic acid (EDTA), tetrahydrofuran (THF), hydroquinone, sodium NaOH were CP and purchased from Sino Pharm Chemical Reagent limited corporation (China), and we made use of those untreated reagents. According to the literatures, 4-cyanopentanoic acid dithiobenzoate (CTA) was prepared [25,26]. Portland cement 42.5R was supplied by the Tianjin cement plant (China).

Characterization of Structure

The structure was characterized by Thermo Nicolet-FT-IR-5700 and Bruker AVAN300CE. The sample for ^{1}H NMR was prepared in deuterium oxide (D_2O). The molecular of SP was assessed by Jasco liquid chromatograph (Tokyo, Japan) GPC Waters 515. Thermal stability of the SP was determined by Thermo Gravimetric Analyzer (TGA, SDTA85/e, Switzerland Metro-Toledo Co., Ltd.).

Fluidity Tests of the Cement Pastes

With reference to GB/T 8077-2000, "methods for testing the uniformity of a concrete admixture," the samples were prepared with a water/cement ratio of 0.29. The SP was added to the water in advance according to the mass of cement pastes. The cement was added to the water and was stirred for 5 min. Then, the cement paste should be pured into a minislump cone. The cone was raised rapidly, and the fluidity of the cement paste was indicated by the spread diameter on the plate.

Adsorption Measurement

The dispersibility of SP in cement pastes is manifested by the absorbance of SP under different wavelength scanning. In the absorption curve, generally chose the largest absorption wavelength lambda λ_{max} to determine the concentration [27]. The adsorption of SP was characterized by PerkinElmer lambda75.

Accurately, the cement paste was 3 g, a certain concentration of SP solution was 9 mL. The cement paste was mixed with SP solution at 25°C for 4 min. When the adsorption reached equilibrium, the fluid of cement paste and SP were taken supernatant fluid by centrifugal separation at 4000 rpm for 10 min. Using UV spectrophotometer determined the concentration of a fluid. Then the adsorption of SP was calculated according to the concentration difference before and after the concentration of fluid adsorption for the powder on the absorption of SP.

Zeta Potential

The Zeta potential of cement was measured by Zetasizer Nano-ZS 90. Dissolved 0.25 g cement with different dosages of the SP was mixed for 5 min [28]. The water/cement (W/C) ratio of the mixture was 40/1 and superplasticizer/cement (SP/C) was 0.29.

Compressive Strength

The compressive strength was measured after 3 and 7 days followed the standard JGJ/T 55-2011 to reveal the effects of the SP on the cementitious strength with the cement (C), fly ash (FA), water (W), sand (S) and aggregate (G) were kept at 1.6, 0.4, 0.78, 4.0, and 5.0 kg. The cubic specimens of the cement pastes with the dimensions of 70 mm × 70 mm × 70 mm were used for the strength measurement.

Isothermal Calorimetry

Isothermal calorimetry tests were evaluated by TAM Air calorimeter (Thermometric AB, Sweden) . Cement pastes were prepared at 20°C. The 0.15% SPs were added to cement pastes. Before the tests, the equipment was set at 20 ± 0.02°C and then maintain for 8 h. Then, 6 g sample was added into a 20 mL sample chamber and then put into the equipment. The heat evolution was recorded for 3 days.

SEM Morphology

The SEM morphology of cement paste was investigated by Zetasizer Nano-ZS 90. The samples were coated with gold by the metalling machine.

Synthesis of the NCM, MPNCM and SP

SP was prepared from SMAS, *N*-carbamoyl maleimide (NCM) and *N*-methoxy polyethylene glycols -*N*'-carbamoyl maleimide (MPNCM) through aqueous graft polymerization. NCM was prepared by MAH and UREA. MPNCM was prepared from NCM and MPEG. The reaction equation for the preparation of NCM, MPNCM, and SP were as follows. For example, NCM was prepared as follows: (6.11 g, 0.1 mol) UREA and 50 mL ET were added to the 250 mL flask. When its temperature was about 40°C, the 20 mL 10 wt % NaOH ethanolic solution, 50 mL ET and 8.82 g, 0.09 mol) MAH were mixed and put dropwise to the reaction system in 30 min. The reaction was at 60°C for 3–8 h. After cooling, filtration, washing by ET and drying, (12.01 g, 0.86 mol) NCM was acquired, the yield rate was 95.3%.

After we obtained NCM, MPNCM was prepared. The 7.1 g, 0.051 mol NCM, (0.34 g, 1.61 mmol) EDTA, (0.51 g, 1.95 mmol) PPh_3, and 50 mL THF solution were thrown into the flask with stirring. When the temperature was 40°C, the (26.1 g, 0.052 mol)

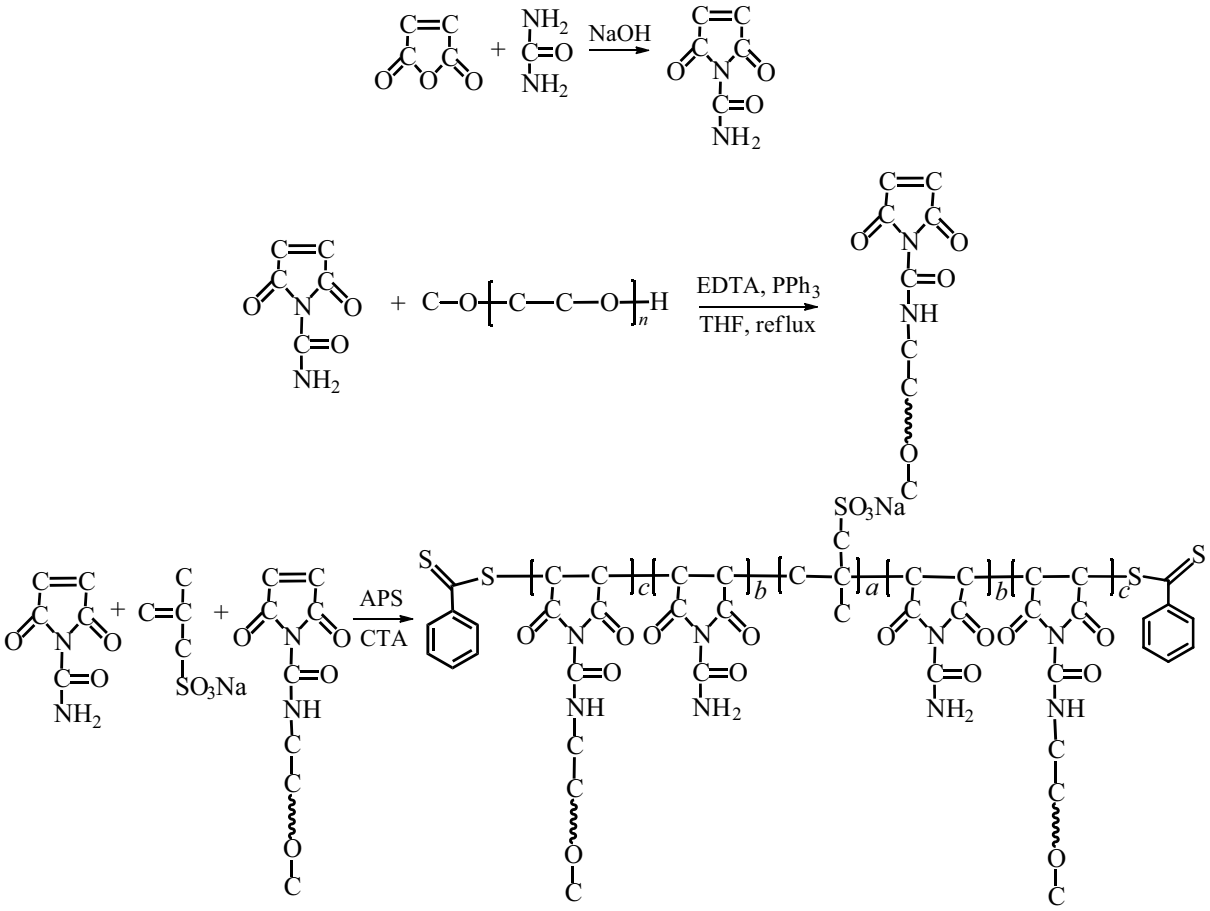

Fig. 2. The equations of reaction.

MPEG were dissolved in 80 mL of THF, and were put dropwise to the reaction system in 30 min. Then, the reaction was at 70°C, for 24 h. After cooling to ambient temperature, the purification of MPNCM was made by rotary evaporator and washed by ET. MPNCM (30.26 g, 0.047 mol) was acquired, and the yield rate was 92.7%.

CTA was prepared as follows: 4,4'-azoblis(4-cayanopentanoic acid) (2.8 g, 10 mmol) and di(thiobenzoyl)disulfide (3.1 g, 10 mmol) were added distilled 80 mL ethylacetate in round-bottomed flask. The reaction solution was heated at reflux for 18 h. Then, the ethylacetate was removed in vacuo. The crude product was isolated by column chromatography using ethyl acetate hexane [29].

After we obtained NCM and MPNCM, SP was prepared. The CTA (0.142 g, 0.46 mmol), APS (0.21 g, 0.92 mmol) were mixed in a 250 mL three-neck round-bottom flask with 150 mL distilled water, which was sealed with a rubber septum and purged with nitrogen for 25 min. When its temperature was about 80°C, MPNCM (15.13 g, 23 mmol) NCM (1.3 g, 9.2 mmol), and SMAS (1.98 g, 13.8 mmol) were assed sequentially, one at a time and at intervals of about 60 min. After 2 h at 80°C, the reaction was essentially complete. Then the hydroquinone (0.05 g, 0.46 mmol) was added to the flask and stirred for 20 min. The purification of SP controlled pH to 6.0 with 10 wt % NaOH solution. Afterward, 200 mL of ET were added thereto so as to precipitate the SP, It was obtained by rotary evaporator and washed with ET. The equations of reaction in Fig. 2

RESULTS AND DISCUSSIONS

Characterization of NCM, MPNCM, SP

The chemical structure of NCM, MPNCM, SP was reflected by FTIR in Fig. 3. The data are analyzed as follows: 3485–3347 cm^{-1} was the characteristic absorption band of amino groups and hydroxyl groups. 2923cm^{-1} was the demonstrable peak of methylene

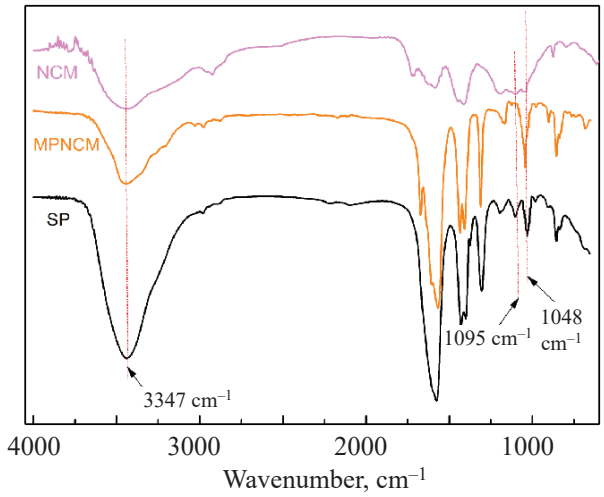

Fig. 3. FI-IR spectrum of NCM, MPNCM, SP.

groups. 1584 cm^{-1} was the stretching vibration of the C=O. 1095 cm^{-1} was the characteristic absorption band of the sulfonate groups. 1048 cm^{-1} was stretching vibration peak of ether bonds [30–32].

Figure 4 shows the ^1H NMR spectrum. As spectrogram(D_2O) showed, δ at 7.07 ppm and 6.61 ppm corresponded to the hydrogen atoms of $–CH_2$ of NCM in Figs. 4a, 4c, 3.66, 3.01, and 3.67, 3.07 ppm were assigned to the hydrogen atoms of $–CH_2$ of MPNCM in Figs. 4b, 4c. Based on the above analysis, the products were certain.

TG-DTG of the SP

Figure 5 shows the TG-DTG spectrum. The thermogravimetric curves of the SP can be depict fore major mass loss steps according to the percentage of weight loss. In the first stage was the increase of temperature from 0 to 91°C and the weight loss of the product was 3.13%, which assigned to the removal of bound and frozen water in the SP. The second stage was the increase of temperature from 91 to 173°C and the weight loss rate of the product was 5.41%, which mainly was the fracture of the SMAS in the SP. The third stage was the increase of temperature from 176 to 226°C and the weight loss rate of the product was 2.52%, which was mainly breakage of the NCM segment in the SP. The fourth stage was the increase of temperature from 226 to 344°C and the weight loss rate of the product was 47.12%, which was mainly breakage of the MPNCM segment in the SP. Finally, the mass loss of the sample tends to be stable over 344°C, and the residual mass of the sample is 54.32%. It was indicated that the scale inhibitor has good thermal

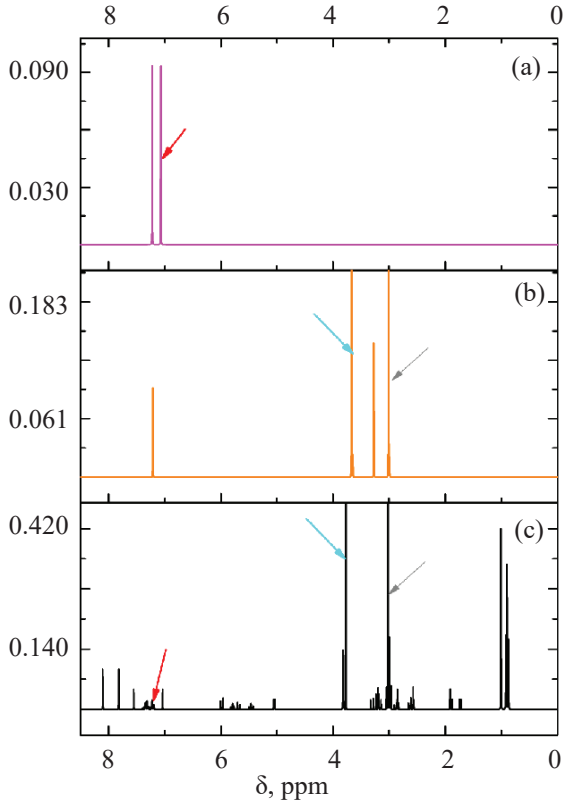

Fig. 4. ^1H NMR spectra of NCM, MPNCM, SP. (a) NCM, (b) MPNCM, (c) SP.

stability when the application temperature of the material is below 91°C. The weight loss rate of NCM, SMAS and MPNCM is very near the reactant ratio, which is confirmed with the data of ^1H NMR mutually.

GPC of the SP

Samples with the different molar ratios of MPNCM : NCM : SMAS, M_n, M_w, PDI and the yield rate, were shown in Table 1. And the GPC spectrum of SP was shown in Fig. 6. Molar of MPNCM is 31.8 g (0.05 mol) .

Table 1. Monomer combination SP

Sample	Molar ratio of MPNCM : NCM : SMAS	M_n	M_w	PDI	Yield rate
SP1	1.00 : 0.20 : 0.80	19152	24860	1.298	98.3%
SP2	1.00 : 0.40 : 0.60	19501	25450	1.305	96.9%
SP3	1.00 : 0.60 : 0.40	18194	23890	1.313	97.6%
SP4	1.00 : 0.80 : 0.20	20450	26320	1.287	97.8%

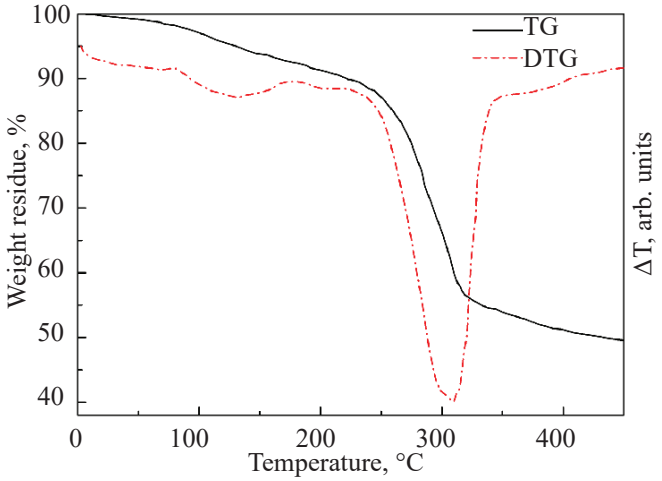

Fig. 5. ^{1}H NMR spectrum of NCM, MPNCM, SP.

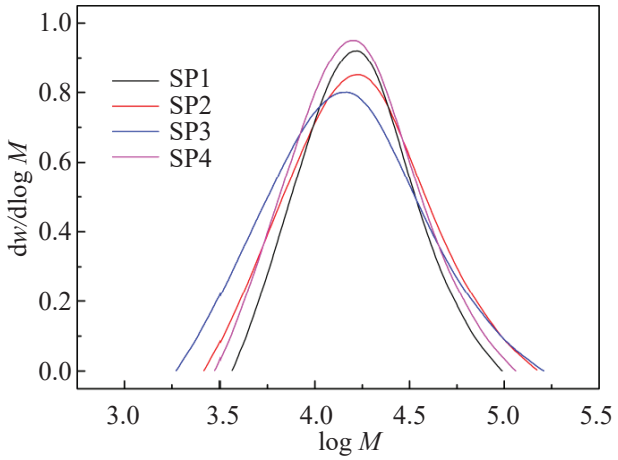

Fig. 6. (Color online) The GPC of the SP.

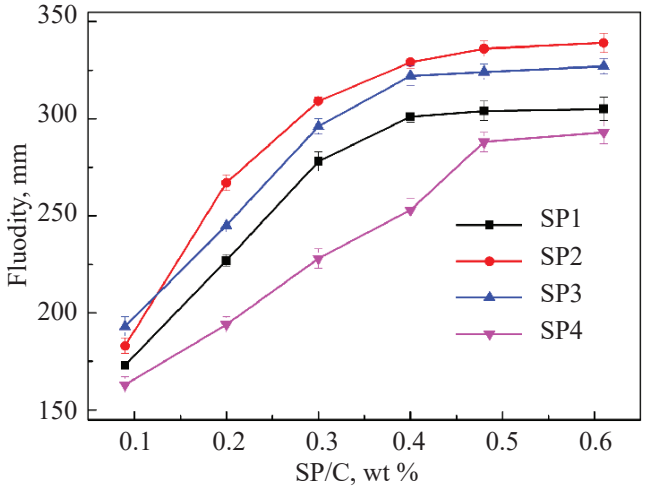

Fig. 7. (Color online) The fluidity of cement pastes with addition of the SP at 0 min (W/C = 0.29) .

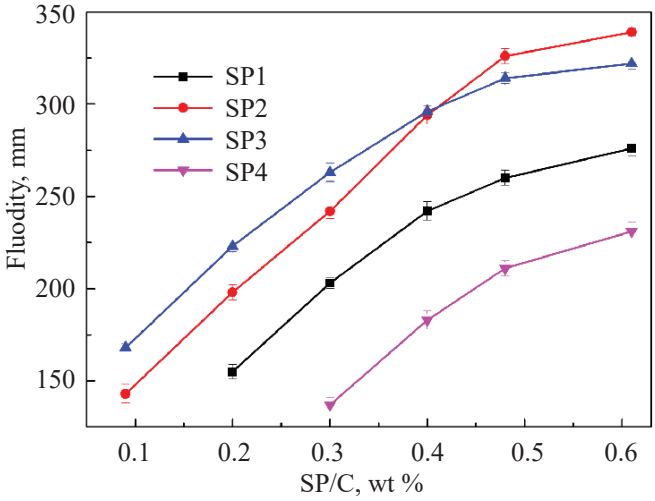

Fig. 8. (Color online) The fluidity of cement pastes with addition of the SP at 60 min (W/C = 0.29) .

Fluidity Tests of the Cement Pastes

A superplasticizer could disperse the cement pastes and improve the performance of concrete. The dispersing and retention capability of SP is evidenced by the fluidity tests of the cement pastes.

Figure 7 illustrates the fluidity of cement pastes at 0 min. The values of the fluidity of cement pastes rapidly increased at 0 min until the optimum effect under the constant value was reached. The transition point appeared at the dosage of about 0.5 wt %.

Figure 8 illustrates the fluidity of cement pastes at 60 min. The values of the fluidity of cement pastes slightly decreased at 60 min. The cement pastes with SP increased the stability of cementitious materials. The fluidity loss occurred, but the effect of time was prolonged and limited. From Figs. 7 and 8, it remains to be seen the sample SP2 presents a good fluidizing effect and retention capability over elapsed time. This indicated that the molar ratio of SMAS, NCM, and MPNCM impacts the dispersing and retention capability of superplasticizers. The synergistic effect of SMAS, NCM, and MPNCM changed the particle surface zeta potential. The repulsive interaction between the cement pastes improved. The fluidity of cement pastes was better.

Adsorption

The adsorption on cement pastes, the electrostatic repulsion and steric hindrance of the superplasticizers

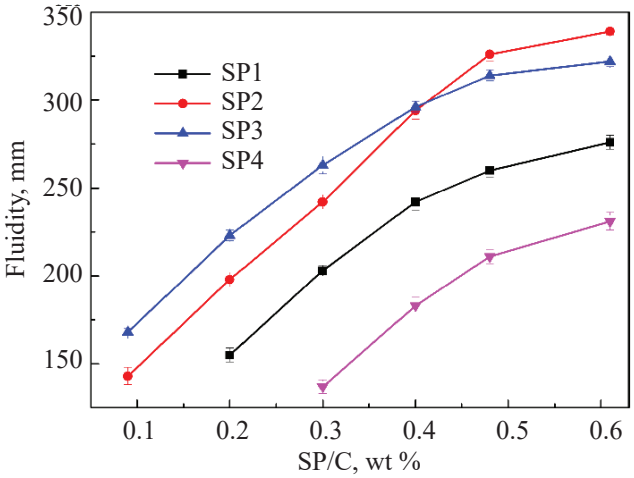

Fig. 9. (Color online) The adsorption of SP on cement pastes (W/C = 0.29).

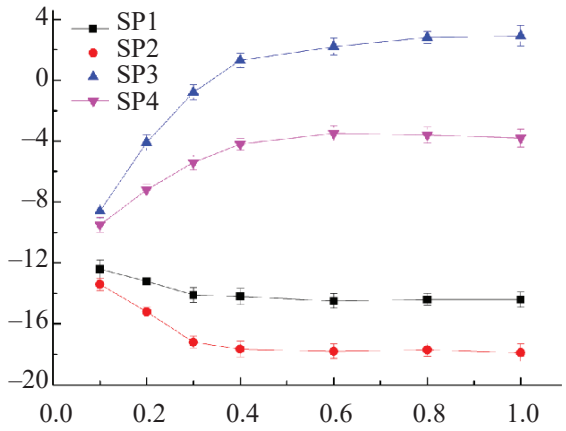

Fig. 10. (Color online) The zeta potential of cement pastes with addition of the SP according to the mass of the cement paste (W/C = 40/1).

and cement pastes effect the dispersing [33, 34]. So it is essential to assess the adsorption and dispersion of the SP. Figure 9 illustrates the adsorption of SP on cement pastes. It is seen the SPs changed the surface charges, such as the negatively charged surface of silicate phases(C_3S and C–S–H) and the positive charges of the surface of the aluminates(C_3A and AFt) [35]. The positive and negative charges of the SP interacted with the charges of the surface of cement pastes are largely responsible for enhancing the flocculation of cement particles with the effects of repulsion of stereo hindrance forming [36]. The saturated adsorption amount changes with the various proportions of SMAS, NCM, and MPNCM on account of the different ratios of the negative and positive charges on the cement particles. The proper ratio of comonomer is benefiting the adsorption.

It is seen that the saturated adsorption amount of SP2 is higher than others. The anionic compound latexes and asphalt emulsions strikingly show the better performance of the adsorption capability than others [8, 37]. When the ratio of SMAS monomer increases, the anionic of SP adsorbed on the surface of cement particles could bridge the effect of Ca^{2+} ions, and improve the capability of the cement pastes. When the ratio of NCM monomer increases, the cationic of SP only interacts with the negatively charged cement surface, but could not unite to form the bridging effect of SO_4^{2-} or OH^- [38].

Zeta Potential

Figure 10 shows the zeta potential of cement pastes with the SP according to the mass of the cement paste (W/C = 40/1). The result indicates that the zeta potential was various from the ratio of SMAS, NCM, and MPNCM monomer. The trend agreed with that in Figs. 7, 8, and 9, the fluidity and adsorption were produced with the ratio of MPNCM, NCM and SMAS increased. Afterward, the zeta potential of SPs was improved with the dosage of SP. When the SP dosage was more than 0.4wt %, the zeta potential became constant. In summary, the SP changed the surface charges, such as the negatively charged and the positive charges with the various ratios of MPNCM, NCM, and SMAS.

It is seen that the zeta potential with added SP was a negative effect in the following: SP2 > SP3 > SP1 > SP4. This illustrated that the adsorbed SP2 could produce more electrostatic repulsions force than the other three samples. The more anionic units in the polymers improve the fluidizing capability than the cationic units. This result shows that a proper ratio of cationic and anionic in the superplasticizers is better for the fluidizing cement pastes than the traditional type of PC superplasticizers [5, 39].

Compressive Strength of Mortar

Figure 11 showed the compressive strength of hardened mortars with SPs. It can be seen from Fig. 11 that comparing with blank, the compressive strength increased after adding SP and showed good workability. Furthermore, the compressive strength of SP2 and SP3 were increased than that of SP1 and SP4. Therefore, SP2 has excellent fluidity and retention ability, which improves the workability of high-performance concrete by using the SP2 [18].

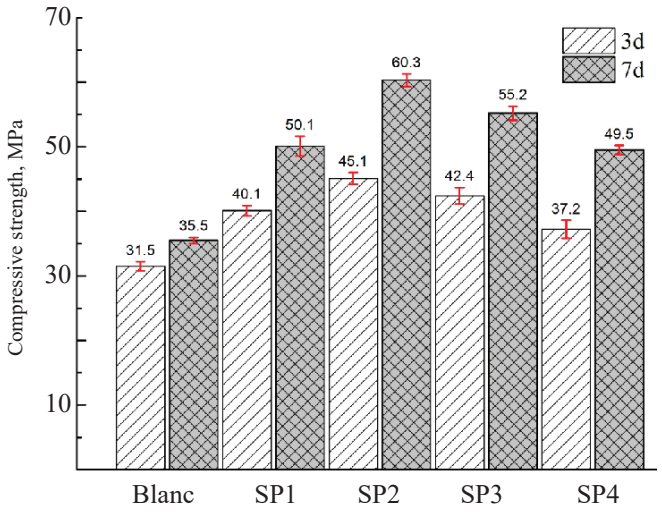

Fig. 11. Compressive strength of SP at dosage of 0.2% and at curing age of 3 and 7 days.

Impacts of Amphoteric SPs on Cement Hydration

Isothermal calorimetry was mirrored by cement pastes to indicate the influences of different SPs on cement hydration (Fig. 12). Based on the previous working theory, the retardation of traditional PCs have failed to be clarified, which investigated by changed induction period and exothermic rate [9]. Compared with previously published data in peer-review journals, reference sample SP1 has unified results in Fig. 12. With the growth of the composition of the cationic units in SP, we could determine from Fig. 12a that the retardation shows less a lower degree of effect. The SP2 show better performance due to the dominating overlapped heat flow curve of the cement paste.

The retardation mechanism of SP has been investigated from both sides as follows. First, the

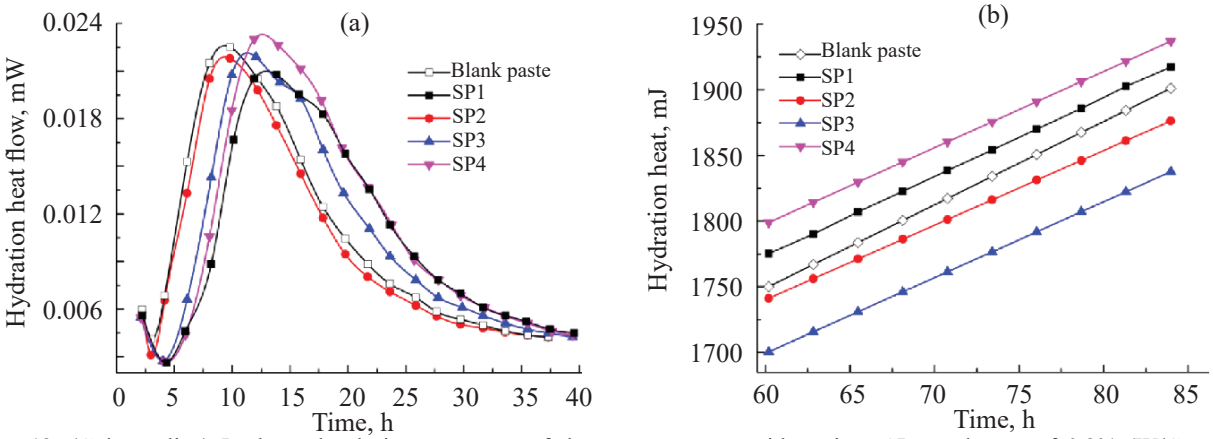

Fig. 12. (Color online) Isothermal calorimetry curves of the cement pastes with various SPs at dosage of 0.2% (W/C = 0.29). (a) Differential heat flow; (b) accumulative heat flow.

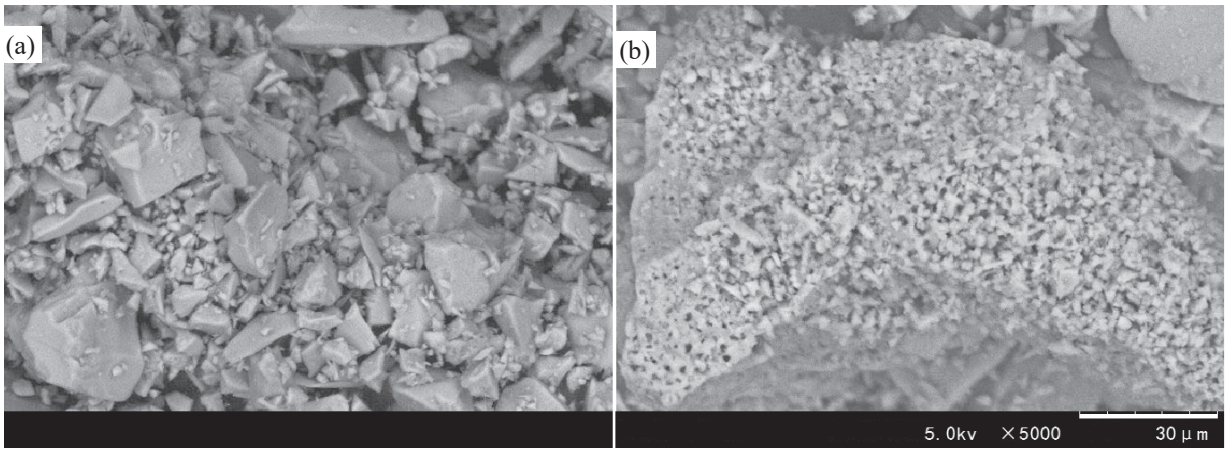

Fig. 13. SEM image of cement hydrated products for 24 h with SP2 at dosage of 0.2% (W/C = 0.29) . (a) Without SP2; (b) with SP2.

adsorption layers of polymer prevent the motion at the interface of cement-solution between solution and solids, which can confirm the physical retardation. Secondly, the SP may further react with Ca^{2+} due to the content of $–SO^{3+}$ and $–NHCO^{–}$ is more than others, which results in either reduction of the concentration of Ca^{2+} in water, or inhibition of nucleation and growth of Ca^{2+} containing hydration products. The latter one could confirm the retardation of chemicals [31]. Nest, the retardation effect of the SPs could be analyzed according to the above views. Then, the adsorption capacity of the SPs is obviously lower than control SP samples. SP2 and the SPs less affect the diffusion process of amphoteric ionic and water bridging with the interface of hydrating solution and solidus. By introducing the cationic group, the content of $–SO_3^{2–}$ in SP is minimized. Hence, the chemical retardation is also weakened.

From Fig. 12b, it is obvious that at age of 3 days, the data is shown in the figure according to SPs, which is lower than the control group. The hydration degree of the SP2 is the lowest. All these results suggest that it is the possibility that introducing the cationic groups into the conventional PC molecules could reduce the retardation effect of SP.

SEM of the Hydrated Products

The morphology of the sample with SP2 at the dosage of 0.2% (W/C = 0.29) was shown in Fig. 13.

Numerous AFt crystals begin to overlap in the needlelike fibrous form in the microstructure photograph of SP2. Meanwhile, the sediment of the C–S–H gel was evenly dispersed among the system. The hydration degree of SP2 as well, owing to the good adsorption. At the early hardening stage, numerous AFt was formed, and its density increases. The SEM demonstrates were also per the results stated before.

CONCLUSIONS

A maleimide-structural copolymer superplasticizer was synthesized by copolymerization of SMAS, NCM, and MPNCM. FTIR measurements confirmed the maleimide structure of the synthesized product. The research results indicated that the maleimide-structural copolymer superplasticizer has better maintenance for cement paste fluidity and concrete slump. It also could affect the surface of cement particles and vary the zeta potential distribution. A suitable addition of cationic units into SP could acquire well performance superplasticizer comparing to the previous research.

FUNDING

This work was supported by Education Commission of Liaoning Province of China (LZGD 2020005), National Natural Science Foundation of China (21706163) and Liaoning Province Department of Education Foundation (LQGD2017020).

CONFLICT OF INTEREST

We declare that we have no conflict of interest.

REFERENCES

1. Lu, S.H., Liu, G., Ma, Y.F., and Li, F., *J. Appl. Polym. Sci*., 2010, vol. 117, no. 1, pp. 273–280.
2. Guo, W.J., Sun, N., Qin, J.J., Zhang, J., et al., *J. Appl. Polym. Sci*., 2012, vol. 125, no. 1, pp. 283–290.
3. Sakai, E., Yamada, K., and Ohta, A., *J. Adv. Concr. Technol*., 2003, vol. 1, no. 1, pp. 16–25.
4. Weng, H.W., Hsu, K.C., and Sheen, Y.N., *J. Appl. Polym. Sci*., 2010, vol. 118, no. 3, pp. 1313–1319.
5. Plank, J., Dai, Z.M., Helena, K., Friedrich, V.H., et al., *Cem. Concr. Res*., 2010, vol. 40, no. 1, pp. 45–57.
6. Yamada, K., Ogawa, S., and Hanehara, S., *Cem. Concr. Res*., 2001, vol. 31, no. 3, pp. 375–383.
7. Tiemyer, C. and Plank, J., *J. Appl. Polym. Sci*., 2012, vol. 124, no. 6, pp. 4772–4781.
8. Ling, J.F, Xiang, M. K., Lu, Z.C., and Hou, S.S., *J. Appl. Polym. Sci*., 2015, vol. 132, no. 4, pp. 78–87.
9. Habbaba, A., Lange, A., and Plank, J., *J. Appl. Polym. Sci.,* 2013, vol. 129, no. 1, pp. 346–353.
10. Manuel, I. and Johann, P., *Ind. Eng. Chem. Res.,* 2019, vol. 58*, no.* 29, pp. 12913–12926.
11. He, Y., Zhang, X., Shui, L.L., and Wang, Y.T., *Constr. Build. Mater*., 2019, vol. 202, no. 1, pp. 656–668.
12. Plank, J., Sakai, E., Miao, C.W., Yu, C., and Hong, J.X., *Cem. Concr. Res*., 2015, vol. 78, part. A, pp. 81–99.
13. Dan, H., Liang, R., Zhao, J., Liu, Z.P., et al., *Constr. Build. Mater*., 2020, vol. 264, no. 4, pp. 120256–120262.
14. Qian, S.S., Yao, Y., Wang, Z.M., Cui, S.P., et al., *Constr. Build. Mater*., 2018, vol. 169, pp. 452–461.
15. Perreira, A.C., Pearson, S., Kostadinova, D., Leroux, F., et al., *Polym. Chem*., 2017, vol. 8, no. 7, pp. 1233–1243.
16. Reddy, K.R., Leel, P.K., and Gopalan, A.I., *J. Nanosci. and Nanotech*., 2007, vol. 7, no. 9, pp. 3117–3125.

17. Stecher, J. and Plank, J., *J. Cem. Concr. Res*., 2019, vol. 119, pp. 36–43.
18. Chen, G., Lei, J.H., Du, Y., Du, X., et al., *Arabian J. Chem*., 2018, vol. 11, no. 6, pp. 747–755.
19. Li, M., Zheng, D.D., and Zhu, Y., *Adv. Cem. Res*., 2017, vol. 29, no. 9, pp. 387–396.
20. Zhang, Y.R., Cai, X.P., Kong, X.M., and Liang, G., *Constr. Build. Mater*., 2017, vol. 155, no. 30, pp. 441–450.
21. He, Y., Zhang, X., Shui, L.L., Wang, Y., et al., *Constr. Build. Mater*., 2019, vol. 202, pp. 656–668.
22. Zhang, K., Pan, L.S., Li, J.C., Lin, C., et al., *Cem Concr. Compos*., 2019, vol. 95, pp. 228–236.
23. Hazer, B., Eren, M., Senemoğlu, Y., Modjinou, T., et al., *J. Polym. Res*., 2020, vol. 27, no. 6, pp. 147–153.
24. Convertine, A.J., Ayres, N., Scales, C.W., Lowe, A.B., et al., *Biomacromolecules*, 2004, vol. 5, no. 4, pp. 1177–1180.
25. Loiseau, J., Ladavière, C., Suau, J.M., and Clacerie, J., *Polymer*, 2005, vol. 46, no. 19, pp. 8565–8572.
26. Favier, A., Charreyre, M.T., and Pichot, C., *Polymer*, 2004, vol. 45, no.26, pp. 8661–8674.
27. Björnström, J. and Chandra, S., *Mater. Struct*., 2003, vol. 36, no. 10, pp. 685–692.
28. Plank, J., Sachsenhauser, B., and Reese, J.D., *Cem Concr Res*., 2010, vol. 40, no. 5, pp. 699–709.
29. Loiseau, J., Ladavière, C., Suau, J.M., and Clacerie, J., *Polymer*, 2005, vol 46, no. 19, pp. 8565–8572.
30. Reddy, K.R., Raghu, A.V., and Jeong, H.M., *Designed Monomers and Polymers*, 2009, vol 12, no. 2, pp. 109–118.
31. Zhang, Y.P., Lee, S.H., Reddy, K.R., Gopalan, A.I., and Lee, K.P., *J. Appl. Polym. Sci*., 2007, vol 104, no. 4, pp. 2743–2750.
32. Hazer, B., Arslan, H., and Senemoğlu, Y., *J. Polym. Res.*, 2019, vol 26, no. 5, p. 101.
33. Miao, C.W., Ran, Q.P., Liu, J.P., Mao, Y.L., et al., *Polym. Polym. Compos*., 2011, vol. 19, no. 1, pp. 1–8.
34. Zhang, D.F., Ju, B.Z., Zhang, S.F., and Yang, J.Z., *J. Appl. Polym. Sci*., 2007, vol. 105, no. 2, pp. 486–491.
35. Plank, J. and Hirsch, C., *Cem. Concr. Res*., 2007, vol. 37, no. 4, pp. 537–542.
36. Yamada, K., *Cem. Concr. Res*., 2011, vol. 41, no. 7, pp. 793–798.
37. Ye, Y.S., Hung, H.L., and Kung, K.C., *J. Appl. Polym. Sci*., 2006, vol. 100, no. 3, pp. 2490–2496.
38. Nakajima, Y., Goto, T., and Yamada, K., *J. Am. Ceram. Soc*., 2005, vol. 88, no. 4, pp. 850–857.
39. Weng, W.K., Hsu, K.C., and Sheen, Y.N., *J. Appl. Polym. Sci*., 2010, vol. 118, no. 3, pp. 1313–1319.